*Proc. Natl. Acad. Sci. USA*
Vol. 90, pp. 9664–9667, October 1993
Chemistry

# Soft x-ray magnetic circular dichroism: A probe for studying paramagnetic bioinorganic systems

(x-ray absorption spectroscopy/*Pyrococcus furiosus*)

J. VAN ELP*, S. J. GEORGE†, J. CHEN*, G. PENG†, C. T. CHEN‡, L. H. TJENG‡, G. MEIGS‡, H.-J. LIN‡, Z. H. ZHOU§, M. W. W. ADAMS§, B. G. SEARLE¶‖, AND S. P. CRAMER*†**

*Energy and Environment Division, Lawrence Berkeley Laboratory, Berkeley, CA 94720; †Department of Applied Science, University of California, Davis, CA 95616; ‡AT&T Bell Laboratories, Murray Hill, NJ 07974; §Department of Biochemistry and Center for Metalloenzyme Studies, University of Georgia, Athens, GA 30602; and ¶Department of Applied and Solid State Physics, Material Science Center, University of Groningen, Nijenborgh 4, 9747 AG Groningen, The Netherlands

*Communicated by Harry B. Gray, July 6, 1993*

**ABSTRACT** **Soft x-ray magnetic circular dichroism was used to study a paramagnetic bioinorganic system. We measured the Fe *L* edges of *Pyrococcus furiosus* rubredoxin, using circularly polarized synchrotron radiation, a split-coil superconducting magnet, low sample temperatures, and fluorescence detection. The observed dichroism effect is strong (30%) and in general agreement with the calculation. The method is element- and oxidation state-specific, and the data can be interpreted by established theoretical procedures. Soft x-ray magnetic circular dichroism demonstrates enormous potential as a probe for studying paramagnetic systems in biology, chemistry, and material science.**

Because of the unique capabilities for investigating the magnetic and electronic structure of 3*d* transition metal and rare earth compounds, soft x-ray magnetic dichroism has attracted considerable attention. Much is due to the recent availability of high flux and resolution and a high degree of linear or circular polarization from synchrotron radiation beamlines in this energy range (200–1500 eV). Here we report soft x-ray magnetic circular dichroism experiments on a paramagnetic bioinorganic system, using the Fe *L* edges of *Pyrococcus furiosus* rubredoxin. Soft x-ray magnetic dichroism was predicted theoretically for the transition metal $L_{2,3}$ edges and the rare earth $M_{4,5}$ edges by Thole *et al.* (1) using atomic multiplet calculations, after which a soft x-ray magnetic linear dichroism effect was found experimentally at the terbium $M_5$ edge in terbium iron garnet (2). Soft x-ray magnetic circular dichroism effects were demonstrated on the $L_3$ and $L_2$ edges of Ni (3, 4) and other 3*d* transition metals (Co and Fe) (5) as well as ferromagnetic and ferrimagnetic oxides (5, 6) and in 3*d* transition metal thin films on Cu (7, 8). A smaller magnetic circular dichroism effect (≈0.5%) was reported in the hard x-ray range at the Fe *K* edge (9). A powerful sum rule, based on the integrated soft x-ray magnetic circular dichroism response of a core level, has been derived recently (10), which allows one to determine the "shell-specific" orbital angular momentum in the ground state.

The potential importance of the soft x-ray magnetic circular dichroism technique extends well beyond the bulk ferromagnets or ferrimagnets to which it has been applied to date. For these systems it has helped to probe the relative spin orientation of different metals or oxidation states, as shown for the tetrahedral and octahedral sites in the Li- and Co-substituted $Fe_3O_4$ spinel (5) and in gadolinium iron garnet (6). Since mixed valence and mixed metal clusters are important catalysts in chemistry and biology, similar studies of paramagnetic metal centers in inorganic compounds or metalloproteins can be of great value for determining the metal cluster electronic structure and magnetic interactions. In materials science, 3*d* transition metal impurities in a metal or semiconductor host can be studied as well as the magnetic interactions between transition metal multilayers. The technique is element specific and only sensitive to the paramagnetic center (a diamagnetic component will not show an effect) of the metalloprotein or inorganic material, thereby increasing the specificity of *L* edge spectroscopy for complex systems. However, in contrast with the concentrated ferro- or ferrimagnets studied to date, orientation of the magnetic moment of a dilute paramagnetic ion requires a strong magnetic field (on the order of several Teslas) and low temperatures, and fluorescence detection is needed to measure the absorption.

The origin of the magnetic dichroism in the rare earth $M_{4,5}$ edges ($3d \rightarrow 4f$ transitions) and the 3*d* transition metal $L_{2,3}$ edges ($2p \rightarrow 3d$ transitions) relies on the nonuniform occupation of the Zeeman-split levels in the initial state, and the effect is a consequence of the selection rules for electric-dipole ($\Delta J = -1, 0, +1$) transitions from the ground state to the final states. For a purely atomic $Fe^{3+}$ high-spin $d^5$ configuration, the ground state is $^6S$, with $L = 0$, $S = 5/2$, and $J = 5/2$. In an applied magnetic field, the ground state is split into six Zeeman levels, for which at $T = 0$ K only the lowest level with $M_J = -5/2$ is occupied. The selection rules for right ($\Delta M_J = -1$) and left ($\Delta M_J = +1$) circularly polarized light allow for right circular polarization only transitions to $J' = 7/2$ final states, since these are the only ones that contain the $M_{J'} = -7/2$ sublevel (see Fig. 1). Excitation with left circularly polarized light is allowed to $J' = 7/2$, 5/2, and 3/2 final states. For the rare earths, the energy variation of $J'$ results in a strong polarization dependence for magnetically ordered materials (1, 11). For the biochemically important 3*d* transition metals, ligand field effects have to be taken into account, but large dichroism effects are still expected (12), and strong soft x-ray magnetic dichroism has been observed in Fe garnets (5, 6).

## MATERIALS AND METHODS

**Sample Preparations.** *P. furiosus* protein is an extremely heat-stable protein (13) recently obtained from an organism that grows optimally around 100°C (14). It was purified by published procedures (13). Samples for this experiment were prepared as partially dehydrated thin films made in an anaerobic glove box by placing about 0.1 ml of 5.0 mM protein in 10 mM Tris·HCl buffer (pH 8.0) on a silicon slide.

**Soft X-Ray Magnetic Circular Dichroism Experiments.** The experiments were carried out with the AT&T Bell Laboratories U4B Dragon beamline (15, 16) located at the National

The publication costs of this article were defrayed in part by page charge payment. This article must therefore be hereby marked "*advertisement*" in accordance with 18 U.S.C. §1734 solely to indicate this fact.

‖Present address: Daresbury Laboratory, Warrington WA4 4AD, United Kingdom.
**To whom reprint requests should be addressed.

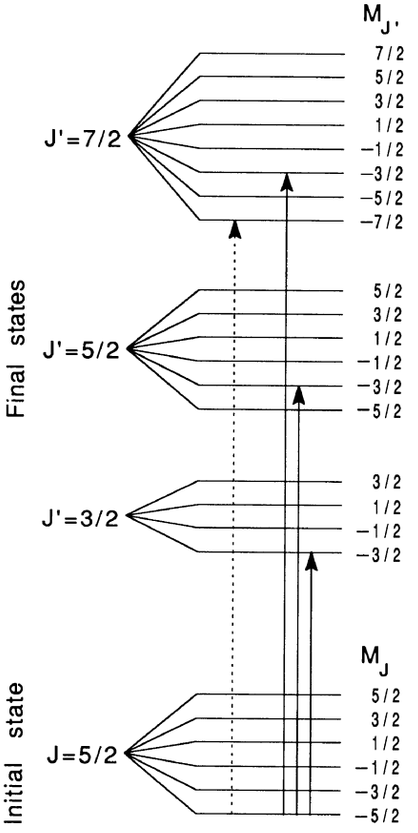


FIG. 1. Soft x-ray magnetic circular dichroism transitions for an atomic $d^5$ configuration. The dashed line is for right circularly polarized light, and the solid line is for left circularly polarized light.

Synchrotron Light Source. This beamline has recently been upgraded to a double-headed configuration, which produces soft x-ray beams of left and right helicity at the same time (17, 18). For these measurements the polarization of these beams was set to around 80%.†† A rotating lateral chopper allowed left or right polarized light to reach the sample, which enabled both spectra to be measured almost simultaneously. The entrance and exit slits were each set to 50 $\mu$m, yielding a calculated energy resolution of $\approx$0.4 eV. The sample was placed at the bottom of a separate cryostat in the center of a split-coil, cold-bore, and ultrahigh vacuum-compatible superconducting magnet. The separate cryostat enables temperature control over a range up from as low as 1.5 K, achieved by adjusting the pumping rate on the liquid helium in the cryostat. Such low temperatures are needed for the alignment of the magnetic moment of a paramagnetic ion or cluster. In the experiments a magnetic field of 4 T was used, and the sample holder was cooled to 1.5 K, although the actual temperature of the sample could be slightly higher. Since the strong magnetic field and the low Fe concentration in metalloproteins make conventional total electron yield or sample photocurrent detection nearly impossible, we have instead used a windowless 13-element Ge solid-state array fluorescence detector (19) positioned in between the coils. By using fluorescence detection, we can electronically resolve the Fe $L$ edge fluorescence from the large, mainly oxygen $K_\alpha$ background, improving the base-line stability and signal-to-noise ratio. In addition, emitted fluorescence photons are not sensitive to the applied magnetic field.

**Data Analysis.** The soft x-ray magnetic circular dichroism spectra shown in Fig. 2 *B* and *C* are the sum of four data sets in which, besides the direction of the magnetic field, also left and right polarization are switched by interchanging both mirrors of the double-headed Dragon beamline. Before each data set was taken, we moved to a new part of the sample to minimize the absorption intensity from photoreduced rubredoxin. After each dichroism experiment, zero field scans were taken for both beams with left and right polarization for calibration purposes. We corrected for an energy offset

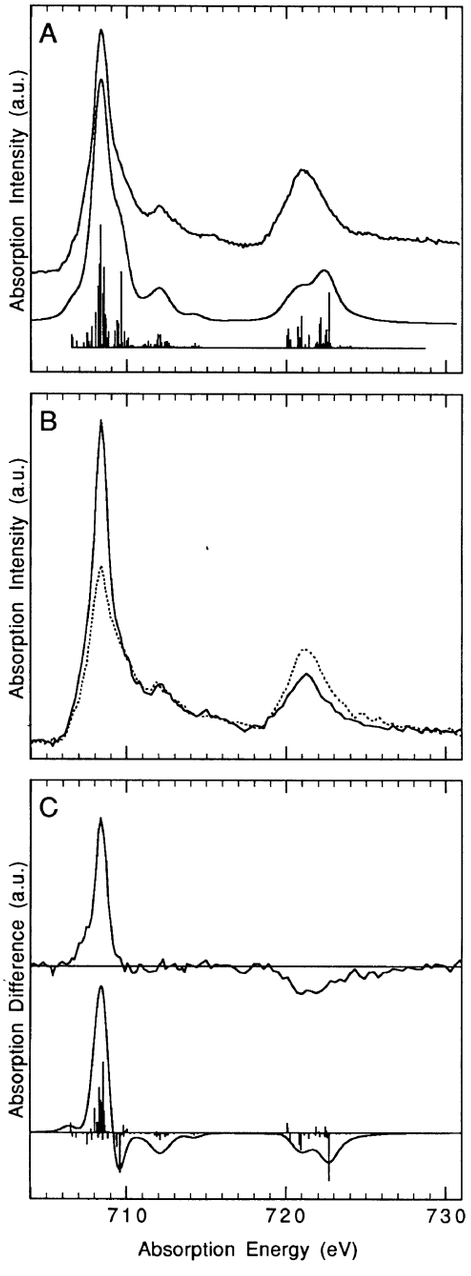


FIG. 2. (*A*) Isotropic spectrum (upper trace) of the oxidized form of *Pyrococcus furiosus* rubredoxin, together with the ligand field atomic multiplet calculation (lower trace). (*B*) The right (solid line) and left (dashed line) circular polarized spectra. (*C*) The experimental (upper trace) soft x-ray magnetic circular dichroism spectrum (right minus left circularly polarized light) and the calculated spectrum (lower trace). The "sticks" shown in *A* and *C* determine the strength of the individual calculated transitions before linewidth broadening. a.u., Arbitrary units.

††For the Fe $L$ edge, the 80% polarization is based on a calculation using an offset angle of $\pm$0.5 milliradian below and above the orbit plane, with an acceptance angle of 0.44 milliradian. The calculated value has been experimentally confirmed at photon energies around 650 eV to be nearly identical to that of the actual value, determined with a crystal polarimeter.

between the two beams of ≈0.1 eV. All four data sets were aligned and the subsequent dichroism effects showed the same energy position, validating our data analysis procedure. For simplicity we will refer in the figure to left and right circular polarization, although the middle two spectra (Fig. 2*B*) are averages of different polarizations and magnetic field directions.

## RESULTS AND DISCUSSION

A strong soft x-ray magnetic circular dichroism effect is observed as shown in Fig. 2. We see a very sharply peaked 30% effect [as defined by $I_{(L-R)/(L+R)}$, where L = left and R = right circular polarizations] at the $L_3$ edge and a rather broad negative structure at the $L_2$ edge. The experimental dichroism intensity at 707 eV is a result of some reduced $Fe^{2+}$ present in the sample, as this shoulder increased during prolonged experiments. The position of the reduced peak corresponds exactly to that observed in an earlier study of reduced and oxidized rubredoxin (20). The calculations were performed by the same method as used by van der Laan and Thole (12). This involves the calculation of reduced matrix elements for the initial ($3d^5$) and final state $2p^53d^6$ configurations in spherical symmetry by using Cowan's atomic multiplet approach (21). A tetrahedral field was used to represent the local $Fe^{3+}$ rubredoxin environment, and the magnetic field reduces this symmetry to $S_4$. The Slater integrals and the $10Dq$ value used were taken from a simulation (20) of the isotropic spectrum, shown in Fig. 2*A*. A symmetry distortion or small changes in the parameters changed the magnetic circular dichroism spectrum only slightly. The core-hole lifetime was taken into account by convolution of the $L_3$ ($L_2$) edge multiplets with a Lorentzian of 0.5 (1.0) eV, and a Gaussian convolution of 0.3 eV was used to simulate the experimental resolution. The main differences between the calculation and the experimental data are found at the high energy side of the $L_3$ and $L_2$ edges. The dichroism features between 710 and 712 eV ($L_3$ edge) are absent in the experimental data, while the observed dichroism at 725 eV ($L_2$ edge) is absent in the calculation. The stick diagram of the calculation shows the strong multiplet effects, characteristic of the $3d$ transition metal edges. Although there is reasonable agreement between the calculation and the isotropic spectrum, as shown in Fig. 2*A*, the measured absorption around 712 eV is stronger than calculated because transitions to $2p^53d^7\underline{L}$ final states (where $\underline{L}$ stands for a ligand hole) have not been considered in the calculations. For $Ni^{2+}$ compounds, comparable satellite features can be obtained in a cluster or impurity calculation (22), in which charge transfer from the ligands to the metal ion is taken into account. In analogy to $3d^6$ to $2p^53d^7$ transitions (12), we expect that satellite states of mainly $2p^53d^7\underline{L}$ character have a mainly positive magnetic circular dichroism contribution at the $L_3$ edge and a mainly negative contribution at the $L_2$ edge. The absence of a dichroism effect at the high-energy side of the $L_3$ edge would result from cancellation by terms of opposite sign. All of the dichroism signal above 725 eV, where the calculation shows almost no spectral weight, would be entirely due to the satellite structure. Since the ligands of the Fe ion in rubredoxin are sulfur atoms, this system is expected, as shown for the $Ni^{2+}$ compounds (22), to be much more covalent than a similar system with, for instance, oxygen ligands. In the calculation this covalency shows up in the smaller values for the reduced Slater integrals, 65% ($3d$–$3d$) and 72.5% ($2p$–$3d$).

The oxidized rubredoxin Fe site is an $S = 5/2$ system. EPR spectroscopy on a structurally comparable rubredoxin has shown the zero-field splittings pattern to be almost completely rhombic with $D = 1.76\ cm^{-1}$ and $E/D = 0.28$ (23). At zero field the ground level is a mixture of $M_J = \pm 5/2$, $\pm 3/2$ and $\pm 1/2$ components. In the Zeeman limit, on the other hand, we find an $M_J = -5/2$ ground state. The calculated dichroism effect for the $L_3$ edge with an $M_J = -5/2$ ground state is 43% [$I_{(L-R)/(L+R)}$]. In the calculations the $M_J = -3/2$ component shows a smaller dichroism effect (about 50% of the $M_J = -5/2$) but an almost identical spectrum because of the weak ligand field-induced $3d$ spin–orbit coupling. Although the applied magnetic field is not strong enough to achieve a full Zeeman-like splitting, the strong experimental dichroism effect presented, taking into account the 80% circular polarization of both photon beams, supports the assumption of a mainly $M_J = -5/2$ ground state.‡‡

In conclusion, we have observed a strong soft x-ray magnetic circular dichroism effect in a dilute paramagnetic bioinorganic system, using a circularly polarized synchrotron radiation source, fluorescence detection, a superconducting magnet, and low temperatures. The dichroism effect observed for rubredoxin is in general agreement with the calculation. Comparison of observed dichroism effects with calculations allows analysis of the orientation of the magnetic moment. In the next few years several third-generation synchrotron radiation sources with specialized insertion devices for circular polarization (24) and an increased photon flux and stability will become operational, significantly increasing the sensitivity of this technique. Thanks to the strong effect we have observed, $L$ edge soft x-ray magnetic circular dichroism studies of paramagnetic clusters in dilute metalloproteins, along with temperature- and magnetic field-dependent experiments, will be feasible. Soft x-ray magnetic circular dichroism, with its sensitivity to relative magnetic orientations of different species and with its straightforward theoretical interpretation, is a promising new probe for bioinorganic and other paramagnetic systems.

‡‡A rough calculation assuming a 50% smaller effect for the $M_J = -3/2$ as compared with the $M_J = -5/2$ and neglecting other levels finds ≈70% $M_J = -5/2$ character for the ground state. This is in reasonable agreement with the orientationally averaged wavefunctions when the published zero-field splitting and a second-order spin Hamiltonian are used.

We thank B. T. Thole, G. van der Laan, G. A. Sawatzky, F. Sette, and E. I. Solomon for useful discussions, interest, and encouragement. This work was supported by National Science Foundation Grants DIR-9105323 and DMB-9107312 (to S.P.C.), Grant DMB-88-05-255 (to M.W.W.A.), National Institutes of Health Grant GM-44380 (to S.P.C.), and Lawrence Berkeley Laboratory Exploratory Research Funds (to S.P.C.). Support from the Netherlands Foundation for Chemical Research and the Committee for European Development of Science and Technology (to B.G.S.) is also acknowledged. The Center for Metalloenzyme Studies at the University of Georgia is funded by a grant from the National Science Foundation (DIR-9014281), and the National Synchrotron Light Source is supported by the Department of Energy under Contract DE-AC02-76CH00016.

1. Thole, B. T., van der Laan, G. & Sawatzky, G. A. (1985) *Phys. Rev. Lett.* **55,** 2086–2088.
2. van der Laan, G., Thole, B. T., Sawatzky, G. A., Goedkoop, J. B., Fuggle, J. C., Esteva, J.-M., Karnatak, R., Remeike, J. P. & Dabkowska, H. A. (1986) *Phys. Rev. B* **34,** 6529–6531.
3. Chen, C. T., Sette, F., Ma, Y. & Modesti, S. (1990) *Phys. Rev. B* **42,** 7262–7265.
4. Chen, C. T., Smith, N. V. & Sette, F. (1991) *Phys. Rev. B* **43,** 6785–6787.
5. Sette, F., Chen, C. T., Ma, Y., Modesti, S. & Smith, N. V. (1990) *AIP Conf. Proc.* **215,** 787–795.
6. Rudolf, P., Sette, F., Tjeng, L. H., Meigs, G. & Chen, C. T. (1992) *J. Magn. Mag. Mat.* **109,** 109–112.
7. Tjeng, L. H., Idzerda, Y. U., Rudolf, P., Sette, F. & Chen, C. T. (1992) *J. Magn. Mag. Mat.* **109,** 288–292.
8. Tobin, J. G., Waddill, G. D. & Pappas, D. F. (1992) *Phys. Rev. Lett.* **68,** 3642–3645.
9. Schütz, G., Wagner, W., Wilhelm, W., Kienle, P., Zeller, R., Frahm, R. & Materlik, G. (1987) *Phys. Rev. Lett.* **58,** 737–740.

10. Thole, B. T., Carra, P., Sette, F. & van der Laan, G. (1992) *Phys. Rev. Lett.* **68,** 1943–1946.
11. Goedkoop, J. B., Thole, B. T., van der Laan, G., Sawatzky, G. A., de Groot, F. M. F. & Fuggle, J. C. (1987) *Phys. Rev. B* **37,** 2086–2093.
12. van der Laan, G. & Thole, B. T. (1991) *Phys. Rev. B* **43,** 13401–13411.
13. Blake, P. R., Park, J.-B., Bryant, F. O., Aono, S., Magnuson, J. K., Eccleston, E., Howard, J. B., Summers, M. F. & Adams, M. W. W. (1991) *Biochemistry* **30,** 10885–10895.
14. Fiala, G. & Stetter, K. O. (1986) *Arch. Microbiol.* **145,** 56–61.
15. Chen, C. T. (1987) *Nucl. Instrum. Methods* **256,** 595–604.
16. Chen, C. T. & Sette, F. (1989) *Rev. Sci. Instrum.* **60,** 1616–1621.
17. Chen, C. T., Sette, F. & Smith, N. V. (1990) *Appl. Opt.* **29,** 4535–4536.
18. Chen, C. T. (1992) *Rev. Sci. Instrum.* **63,** 1229–1233.
19. Cramer, S. P., Chen, J., George, S. J., van Elp, J., Moore, J., Tensch, O., Colaresi, J., Yocum, M., Mullins, O. C. & Chen, C. T. (1992) *Nucl. Instrum. Methods* **319,** 285–289.
20. George, S. J., van Elp, J., Chen, J., Ma, Y., Chen, C. T., Park, J.-B., Adams, M. W. W., Searle, B. G., de Groot, F. M. F., Fuggle, J. C. & Cramer, S. P. (1992) *J. Am. Chem. Soc.* **114,** 4426–4427.
21. Cowan, R. D. (1981) *The Theory of Atomic Structure and Spectra* (Univ. of California Press, Berkeley).
22. van der Laan, G., Zaanen, J., Sawatzky, G. A., Karnatak, R. & Esteva, J.-M. (1986) *Phys. Rev. B* **33,** 4253–4263.
23. Peisach, J., Blumberg, W. E., Lode, E. T. & Coon, M. J. (1971) *J. Biol. Chem.* **246,** 5877–5881.
24. Kim, K.-J. (1990) *SPIE Proc.* **1345,** 116 (abstr.).